Available online at www.sciencedirect.com

ScienceDirect

Proceedings of the Combustion Institute 37 (2019) 469–476

Proceedings of the Combustion Institute

www.elsevier.com/locate/proci

The $C_2H_2 + NO_2$ reaction: Implications for high pressure oxidation of C_2H_2/NO_x mixtures

Paul Marshall [a,*], Caroline Leung [a], Jorge Gimenez-Lopez [b,c], Christian T. Rasmussen [b], Hamid Hashemi [b], Peter Glarborg [b], Maria Abian [c], Maria U. Alzueta [c]

[a] *Department of Chemistry and Center for Advanced Scientific Computing and Modeling, University of North Texas, 1155 Union Circle #305070, Denton, TX 76203-5017, USA*

[b] *DTU Chemical Engineering, Technical University of Denmark, Lyngby DK-2800, Denmark*

[c] *Aragon Institute of Engineering Research I3A, Department of Chemical and Environmental Engineering, University of Zaragoza, Zaragoza 50018, Spain*

Received 29 November 2017; accepted 25 June 2018
Available online 25 July 2018

Abstract

The reaction of C_2H_2 with NO_2 has been studied theoretically. It is a complex overall reaction with multiple wells and multiple product channels. The calculated rate constant for the preferred channel, formation of a CHOCHON adduct, is compatible with the only experimental determination. The CHOCHON adduct is assumed to dissociate rapidly to form the triplet carbene CHCHO and NO. An experimental and kinetic modeling study of the interaction between C_2H_2, O_2 and NO_x was performed under flow reactor conditions in the intermediate temperature range (600–900 K), high pressure (50–60 bar), and for stoichiometries ranging from reducing to strongly oxidizing. The results show that presence of NO_x serves both to sensitize and inhibit oxidation of C_2H_2. Calculations with a detailed chemical kinetic model, partly established in the present work, confirm that $C_2H_2 + NO_2$ is the major initiation step, as well as the major sensitizing reaction. This reaction converts NO_2 to NO, which is then partly converted to HCN by reaction with C_2H_3 and CHCHOH. The latter reactions are both chain terminating and serve as the major inhibiting steps.

Keywords: $C_2H_2 + NO_2$; Ab initio theory; High pressure flow reactor; Sensitization

1. Introduction

Acetylene is an important intermediate in the combustion of most hydrocarbon fuels. Even though the oxidation chemistry of acetylene has been studied extensively in the past [1], results for the low-to-medium temperature oxidation chemistry is mostly limited to early static reactor work

* Corresponding author.
E-mail address: Paul.Marshall@unt.edu (P. Marshall).

https://doi.org/10.1016/j.proci.2018.06.202
1540-7489

[2–5], and few experiments have been conducted at increased pressure [6–9]. In particular, there is little knowledge about the interaction of acetylene with nitrogen oxides. Studies of acetylene/nitrogen oxide interactions have been reported from batch reactors [10], flames [11,12], jet-stirred reactors [13] and flow reactors [14]. Most of these studies [12–14] have addressed reburn type chemistry; i.e., reduction of nitric oxide by reaction with fuel derived radicals. The presence of nitrogen oxides, even in small amounts, may have a significant impact on fuel oxidation characteristics [15], but studies of mutual sensitization in the oxidation of acetylene and NO_x are very limited.

The objective of the present work is to analyze the mutual oxidation of C_2H_2 and NO/NO_2, as well as the capability of acetylene to reduce NO, under high pressure conditions and temperatures below 1000 K. The work involves a theoretical study of the $C_2H_2 + NO_2$ reaction, which is the main initiation reaction in this system, together with an experimental and kinetic modeling study of $C_2H_2/O_2/NO_x$ reaction at high pressure.

2. Theoretical study of $C_2H_2 + NO_2$

The $C_2H_2 + NO_2$ reaction has a significantly lower activation energy than $C_2H_2 + O_2$ and may serve as an important initiation step in oxidation of acetylene in the presence of nitrogen dioxide. However, little is known about this reaction. Thomas [10] studied the reaction in a batch reactor at low pressure and temperatures of 443–493 K, but his determination of the rate constant, corrected in a subsequent paper [16], would be expected to be affected by secondary reactions. Using estimation rules, Sprung et al. [17] calculated the rate constants for addition of NO_2 to selected olefins, proposing a rate constant for $C_2H_2 + NO_2$ about two orders of magnitude faster than the (corrected) value of Thomas [16]. In the absence of a reliable rate constant and set of products for $C_2H_2 + NO_2$, we decided to study the reaction by ab initio methods.

2.1. Method

Initial exploration of the potential energy surfaces (PES) for the interaction of C_2H_2 with NO_2 was made with the CBS-QB3 method [18]. The nature of the transition states was checked via inspection of the intrinsic reaction coordinate and the motion of the normal mode for the single imaginary frequency. Barrierless processes were validated via relaxed scans. This involves characterization of the structure and vibrational frequencies of stationary points with density functional theory (DFT), B3LYP/6-311G(d,p), followed by a series of single-point calculations combined to approximate the coupled cluster CCSD(T) energy at the complete basis set limit. Then the geometries and frequencies of the stationary points were refined with a more accurate functional, M06-2X [19], and larger basis set, 6–311+G(2df,2p). All structures are shown in the Supplementary Material, where also energies are provided. For the purpose of evaluation of the contribution of zero-point vibrational energy to the relative enthalpies at 0 K the frequencies were scaled by a factor of 0.970 [20]. DFT is relatively insensitive to the significant spin contamination in the UHF (spin-unrestricted Hartree–Fock) wavefunction of some of the species. Two further approaches, also chosen to be relatively insensitive to this spin contamination, were applied at these geometries to derive the total energy at the complete basis set limit, E_∞. The first is based on UCCSD(T)/UHF results using the total energies E_3 with the cc-pVTZ basis set and E_4 with the cc-pVQZ basis set. E_∞ was obtained via the relation $E_\infty = (64E_4 - 27E_3)/27$ [21].

The second approach, also implemented at the M06-2X/6-311+G(2df,2p) geometries and then combined with the scaled zero-point energies, is the CBS-APNO method [22]. All calculations were carried out with the Gaussian 09 [23] and 16 [24] programs.

The transition state theory (TST) analysis used M06-2X/6-311+G(2df,2p) moments of inertia and frequencies scaled by 0.944 [20] , and barriers evaluated with CBS-APNO theory. Inspection of the normal modes revealed that the lowest frequency could be treated as a hindered rotor. The TST calculations were implemented with the THERMO routine written by Barker and coworkers [25].

2.2. Discussion

Table 1 summarizes the computed energies and the resulting enthalpies at 0 K, relative to $C_2H_2 + NO_2$. It may be seen that the three CCSD(T)-based methods are in good agreement which lends some support to the idea that deficiencies in the single-determinant UHF wavefunctions have been compensated for here. The worst cases have $<S^2>$ of up to 1.55, much higher than the ideal value of 0.75. This compensation has been noted for CBS-APNO [26], and the CBS-QB3 approach includes an explicit correction term for spin contamination [18]. We also compare to ROCBS-QB3 energies [27], where spin-contamination is eliminated by use of spin-restricted open-shell wavefunctions, and note generally good accord with the CBS-APNO results. The DFT energies are in broad accord, to within ca. 20 kJ mol^{-1}. A measure of the degree of multireference character is the T1 diagnostic [28]. Schaefer and coworkers argued that for open-shell molecules, coupled cluster theory should be reliable for T1 values up to 0.044 [29]. From the values in Table 1 it may be seen that this criterion is exceeded dramatically for the barrier at TS5 and also for TS2. Fortunately, because these barriers are more than 150 kJ mol^{-1} above the reactants, the

Table 1
Expectation values of $<S^2>$, T1 diagnostic and computed enthalpies for species in the $C_2H_2 + NO_2$ system.

Species	State	$<S^2>$	T1 value	Relative enthalpy at 0 K/kJ mol^{-1}				
				M06-2X/ 6–311+G(2df,2p)	CCSD(T)/ CBS	CBS-QB3	ROCBS-QB3	CBS-APNO
NO_2	$^2A_1$	0.77	0.023	0	0	0	0	0
C_2H_2	$^1\Sigma_g$	0	0.013					
Molecule A'[a]	$^2A'$	0.96	0.032	24.5	36.6	35.7	37.3	42.6
Molecule A	$^2A'$	0.96	0.032	20.9	34.0	31.2	32.6	37.5
Molecule B'[a]	$^2A'$	1.21	0.048	–240.0	–213.2	–211.0	–219.5	–211.8
Molecule B	$^2A'$	1.22	0.048	–242.8	–213.8	–224.9	–223.4	–214.7
Molecule C	^2A	0.99	0.036	18.3	32.9	35.6	36.5	39.1
Molecule D	$^2B_1$	0.77	0.025	–124.3	–100.6	–100.7	–100.8	–100.3
Molecule E	$^2A''$	0.78	0.047	–44.0	–9.1	–19.7	–[b]	–22.3
Molecule F	$^2A''$	0.88	0.026	4.1	45.5	36.5	36.6	47.8
NO	$^2\Pi$	0.77	0.021	64.5	82.8	90.5	–[b]	94.2
CHCHO	$^3A''$	2.18	0.034					
TS1	$^2A'$	1.03	0.037	63.5	74.4	67.3	67.5	69.4
TS2	^2A	1.55	0.070	154.8	164.2	154.9	–[b]	162.4
TS3	$^2A'$	0.99	0.042	78.2	86.3	80.3	80.3	80.8
TS4	^2A	1.26	0.053	62.8	68.7	63.6	56.7	67.6
TS5	$^2A'$	1.20	0.052	232.4	249.6	244.4	–[b]	251.4

[a] Higher energy conformer of following molecule.
[b] Calculation did not converge.

conclusion that these pathways are unimportant here is not affected by uncertainty in the exact energies. Similarly, caution must be applied to the energies derived for TS4 and molecule E but this does not change the conclusions below.

Because the CBS-APNO model chemistry has been widely used in the past and evaluated thoroughly, including uncertainties, we select these results for further analysis. Root-mean-square errors of ~4 and 4.2 kJ mol^{-1} have been proposed for bond strengths in hydrocarbons and barrier heights [22,30], respectively. We suggest error limits of ca. 10 kJ mol^{-1} here.

NO_2 can add to acetylene to form a new C–N or new C–O bond. Both steps are similarly endothermic, by about 36 kJ mol^{-1}, but there is a significant barrier so the resulting adducts are metastable. Some subsequent unimolecular chemistry of these species is mapped out in the potential energy diagrams shown in Fig. 1. Because there are large barriers to further isomerization of species A, $CHCHNO_2$, it is unlikely to lead to new chemistry. Species C, CHCHONO, isomerizes readily to a cyclic c-$C_2H_2NO_2$ species D and, because the second barrier is lower than the initial transition state TS3, initially energized CHCHONO may isomerize before collisional stabilization. In turn, there appears to be no barrier beyond the endothermicity for the initially energized cyclic species to undergo ring opening to make CHOCHON, species E. On the assumption that the pre-exponential factor for ring opening via a loose transition state is $A_\infty \approx 10^{16}$ s^{-1} at its high-pressure limit, and that the activation energy E_∞ is 80 kJ mol^{-1}, we can derive energy-specific rate constants k(E) via the inverse Laplace transform. Given that c-$C_2H_2NO_2$ (species D) is initially formed with at least 181 kJ mol^{-1} of excess energy, we calculate k(E) at this threshold to be of the order of 10^{14} s^{-1}. For collisional stabilization to be competitive one would require a density of ca. 10^{24} molecule cm^{-3} or a pressure of ca. 10^5 bar at, for example, 500 K. Thus we propose that CHOCHON is the major product of $NO_2 + C_2H_2$. This species has a small C–ON bond strength of 116 kJ mol^{-1}. This means that NO can easily be eliminated to leave a triplet carbene, especially as the CHOCHON is formed in an initially energized state. Two of many possible reactions the carbene could undergo are with molecular oxygen and nitrogen dioxide, respectively, to make glyoxal. The NO can be oxidized back to NO_2 leading to a catalytic cycle for NO_x.

The rate-determining step for the kinetically favored path shown in Fig. 1 is crossing the initial barrier at TS3 which we compute to be 80.8 kJ mol^{-1}. TST analysis yields the rate constants plotted on Fig. 2. The rate constant is $k_1 = 1.42 \times 10^3$ (T/K)$^{2.79}$ exp(−69.9 kJ mol^{-1}/RT) cm^3 mol^{-1} s^{-1}. Also shown there are experimental kinetics for $C_2H_2 + NO_2$ re-evaluated from the work of Thomas [10]. Thomas determined k_1 from measurements of the NO_2 decay rates in a C_2H_2/NO_2 mixture. We have divided the rate constant from Thomas by 200, arising partly from an error of a factor of 100 as pointed out later by Thomas [16] and partly from an additional factor of two coming from each acetylene molecule removing

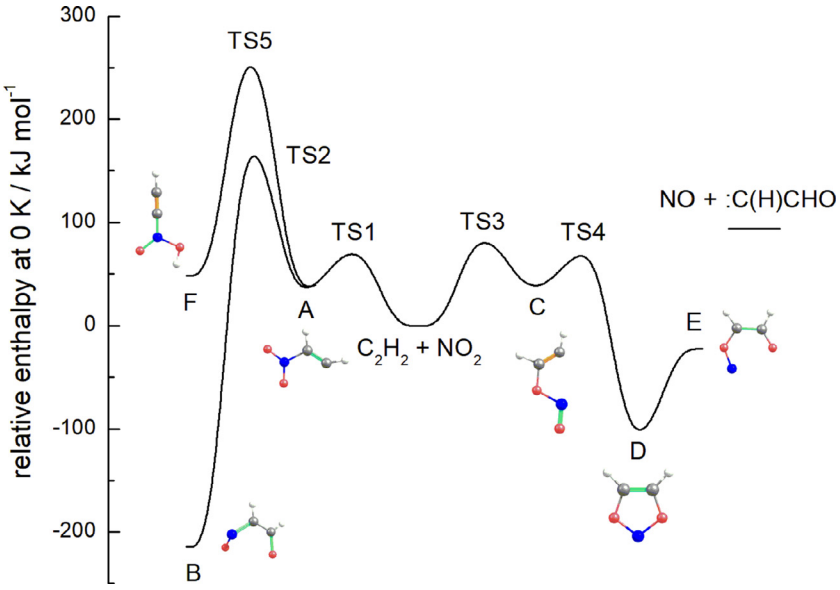

Fig. 1. Potential energy diagram for $C_2H_2 + NO_2$ based on CBS-APNO energies obtained at M06-2X/6-311+G(2df,2p) geometries.

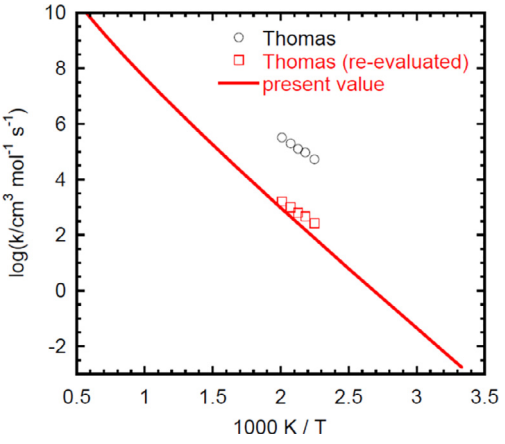

Fig. 2. Arrhenius plot for the $C_2H_2 + NO_2$ reaction. The experimental values (symbols) are the (erroneous) rate constant originally reported by Thomas [10] and the value re-evaluated in the present work (see text). The line denotes the rate constant calculated from TST in the present work.

two NO_2 in the sequence,

$$C_2H_2 + NO_2 \rightleftarrows CHCHO + NO \quad (R1)$$

$$CHCHO + NO_2 \rightleftarrows OCHCHO + NO \quad (R2)$$

As discussed below, the $CHCHO + NO_2$ reaction can be expected to be fast. The accord obtained between TST and experiment is good. The discrepancy, which corresponds to a reduction in the TS3 barrier of ca. 4 kJ mol^{-1}, is well within both the experimental and the computational uncertainty.

The need to treat molecule E, CHOCHON, as a distinct species depends on the temperature range of interest. At 500 K our RRKM calculations indicate that if it is formed "cold" its unimolecular decay would be rapid, with a rate of ~7000 s^{-1} at the high pressure limit, while at 700 K it dissociates with an estimated rate of $2 \cdot 10^7$ s^{-1}. In fact, with the likelihood of considerable internal excitation after passing TS3, it is possible that the wells of C, D and E will be skipped on the way to NO + CHCHO. In the present work, we have assumed that the dissociation to CHCHO and NO is effectively instantaneous.

3. High-pressure oxidation of C_2H_2/NO_x mixtures

3.1. Experimental

The experiments for the C_2H_2-O_2-NO_x interaction were carried out in a laboratory-scale high pressure laminar flow reactor designed to approximate plug-flow. The setup is described in detail elsewhere [31] and only a brief description is provided here.

The reactions took place in a tubular quartz reactor enclosed in a stainless steel tube that acted as a pressure shell. A tube oven with three individually controlled electrical heating elements ensured an isothermal reaction zone (±5 K) of approximately 43 cm, with steep temperature gradients toward both the inlet and outlet of the

Table 2
Selected reactions from the C_2H_2/NO_x subset. Parameters for use in the modified Arrhenius expression $k = AT^{\beta} \exp(-E/[T])$. Units are mol, cm, s, K.

		A	β	E/R	Source
1.	$C_2H_2 + NO_2 \rightleftarrows CHCHO + NO$	1.4E03	2.790	8400	pw,[a]
2.	$CHCHO + NO_2 \rightleftarrows OCHCHO + NO$	5.9E13	0.000	0	est as CH_2+NO_2
3.	$C_2H_3 + NO_2 \rightleftarrows CH_2CHO + NO$	7.7E14	−0.600	0	[34]
4.	$CHCHOH + NO_2 \rightarrow HCO + HCOH + NO$	7.7E14	−0.600	0	est as $C_2H_3+NO_2$
5.	$OCHCHO + NO_2 \rightleftarrows OCHCO + HONO$	1.4E−7	5.640	4640	est as CH_2O+NO_2
6.	$CHCHO + NO \rightleftarrows HCNO + CO + H$	5.0E12	0.000	0	est as CH_2+NO
7.	$C_2H_3 + NO \rightleftarrows HCN + CH_2O$	4.0E13	−0.200	0	[35],[b]
8.	$CHCHOH + NO \rightleftarrows HCN + HOCHO$	4.0E13	−0.200	0	est as C_2H_3+NO (k_∞)

[a] The CHOCHON adduct formed is assumed to dissociate instantaneously.
[b] Est high-pressure limit, assuming A T^{β} format.

reactor tube. Measured temperature profiles for the reactor have been reported elsewhere [32]. High-purity reactant gases, fed from gas cylinders, were premixed before entering the reactor.

Product analysis was conducted with a gas chromatograph (TCD/FID) and a NO_x chemiluminescence gas analyzer. The GC allowed detection of O_2, CO, CO_2, C_2H_6, C_2H_4, C_2H_2, and CH_4 with an overall relative measuring uncertainty in the range ±5%. A similar accuracy was obtained for measurements of NO and NO_2 using the NO_x chemiluminescence gas analyzer. The principle of the NO_2 measurement was by means of a catalytic converter that reduced NO_2 to NO. However, HONO and $HONO_2$ were presumably converted to NO as well by the catalyst and thus we assume that the NO_2 measurement is in fact the sum of $NO_2 + HONO + HONO_2$.

3.2. Detailed kinetic model

The reaction mechanism and corresponding thermodynamic properties were mostly drawn from recent work on high-pressure acetylene oxidation [9] and on nitrogen chemistry [33]. Reactions added in the present work for the C_2H_2/NO_x subset are listed in Table 2; the full mechanism is available as supplementary material.

In addition to $C_2H_2 + NO_2$ (R1), nitrogen dioxide may react with C_2H_3 (R3) and with the oxygenated species CHCHO (R2), CHCHOH (R4), and OCHCHO (R5). The rate constant for $C_2H_3 + NO_2$ was measured by Geppert et al. [34]; for reactions R2, R4, and R5, we rely on analogy to similar reactions. The key reactions involving NO are $C_2H_3 + NO$ (R7) and CHCHOH + NO (R8), both forming HCN. Reaction R7 was studied experimentally and theoretically by Stribel et al. [35]; the rate constant for CHCHOH + NO (R8) is assumed to be similar to k_7.

As discussed above, the $C_2H_2 + NO_2$ reaction (R1) yields triplet formylmethylene (^{3}CHCHO) as the major product. The ^{3}CHCHO radical is a triplet carbene like triplet methylene ($^3CH_2$) and rate constants were assumed to be similar. Consequently, we have estimated the rate constant for CHCHO + NO (R6) to be roughly similar to $CH_2 + NO$. A subset for the ^{3}CHCHO radical was included in the mechanism with estimated rate constants [9].

3.3. Results and discussion

Mixtures of 1000 ppm C_2H_2, 500 ppm NO_x, and O_2, highly diluted in N_2, were reacted at pressures of 50–60 bar and stoichiometries ranging from reducing to oxidizing conditions. The flow rate of 3 L min^{-1} (STP) resulted in (temperature dependent) residence times of 10–15 s in the isothermal zone of the reactor. The diluted conditions ensured a low heat release during the reaction.

In the presence of O_2 a significant fraction of the fed NO was oxidized to NO_2 in the low temperature, high pressure tubing prior to the isothermal zone inside the reactor through the reaction $NO + NO + O_2 \rightarrow NO_2 + NO_2$. The partitioning of NO and NO_2 in the inlet was estimated for each experiment, based on the measured ratio of these species at the lowest investigated temperature. The values obtained this way are in good agreement with those reported by Gimenez–Lopez et al. [32] calculated from kinetic modeling of the inlet system under similar conditions.

Figure 3, which compares data obtained in the present work with those of Gimenez–Lopez et al. [9] obtained under similar conditions, shows the effect of adding NO_x on acetylene oxidation at different stoichiometries. In the absence of nitrogen oxides, the temperature for onset of reaction is about 725 K, independent of stoichiometry. Above this temperature, acetylene is rapidly oxidized, as predicted by the model [9]. Addition of NO_x shifts the onset temperature to values below 600 K. However, upon onset of reaction the oxidation rate in the presence of nitrogen oxides is lower than in the absence of NO_x; this is most pronounced for reducing conditions. From the results of Fig. 3, it is clear that presence of nitrogen oxides both sensitizes and inhibits oxidation.

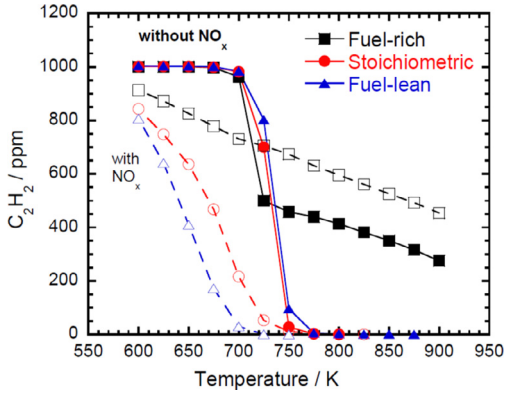

Fig. 3. Comparison of measured concentration profiles for acetylene as a function of the stoichiometry (λ = 0.18/59.6 bar; λ = 0.99/59.6 bar; and λ = 19.4/49.6 bar), the reactor temperature and the NO_x concentration (0 or 500 ppm). The data obtained in the absence of NO_x (closed symbols) are adopted from Gimenez–Lopez et al. [9], while the experiments with addition of NO_x (open symbols) were conducted in the present work. Apart from the level of NO_x, reaction conditions were the same (see following figures).

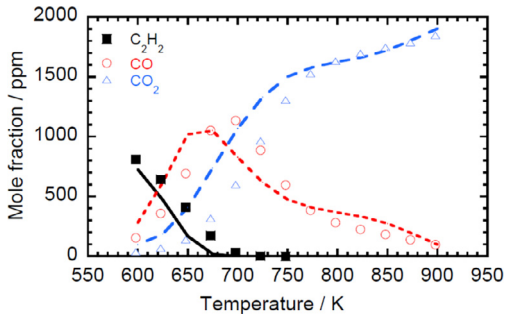

Fig. 4. Comparison of experimental and predicted concentration profiles as a function of the reactor temperature for the oxidizing experiment with C_2H_2/O_2 (λ = 19.4). The pressure was 49.6 bar and the reactor residence time was 7346/T (s · K). The inlet composition was 1000 ppm C_2H_2, 484 ppm NO_x, 4.9% O_2, and N_2 by difference. The symbols mark experimental data while lines denote model predictions obtained at isothermal conditions. In the modeling, all NO_x was assumed to enter the reactor as NO_2.

Figure 4 compares the flow reactor results obtained under very lean conditions (excess air ratio λ = 19.4) with modeling predictions. In the calculations, all the NO supplied by the gas cylinder is assumed to be oxidized to NO_2 in the inlet section. Acetylene is fully consumed at 700 K, where also CO peaks. Above this temperature, CO is gradually oxidized to CO_2. The model predicts the experimental trends well, even though the oxidation rate is slightly overpredicted below 750 K.

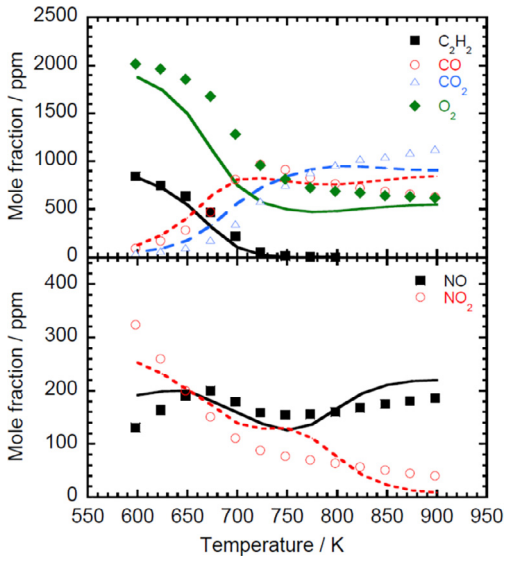

Fig. 5. Comparison of experimental and predicted concentration profiles as a function of the reactor temperature for the stoichiometric experiment with C_2H_2/O_2 (λ = 0.99). The pressure was 59.6 bar and the reactor residence time was 8827/T (s · K). The inlet composition was 1000 ppm C_2H_2, 500 ppm NO_x, 2490 ppm O_2, and N_2 by difference. The symbols mark experimental data while solid lines denote model predictions obtained at isothermal conditions. In the modeling, all NO_x was assumed to enter the reactor as NO_2. Measured NO_2 was taken as the sum of NO_2, HONO, and $HONO_2$.

Due to the large excess of O_2, oxidation of NO would also be expected to occur in the outlet section after the isothermal zone. For this reason no comparison is shown for nitrogen oxides for the lean conditions. However, the observed inlet and outlet total concentrations of NO_x are the same, in agreement with predictions.

Under stoichiometric conditions (Fig. 5), reaction starts below 600 K and acetylene is completely converted to CO and CO_2 at 725 K. Above this temperature, CO is only slowly oxidized to CO_2 despite the presence of O_2. Nitrogen dioxide in the inlet is reduced to NO, which peaks in concentration at around 675 K. Above this temperature, NO is partly reduced, presumably to HCN (not measured). The model captures well the experimental data.

At reducing conditions (λ = 0.18, Fig. 6), the NO to NO_2 ratio in the inlet to the isothermal region of the reactor is uncertain; in the modeling we assumed starting concentrations of 100 ppm NO and 370 ppm NO_2. The experimental data show a steady decline in acetylene and oxygen concentrations with increasing temperature, with CO and, to a minor extent, CO_2 concentrations increasing. At lower temperatures, NO increases due to reduction of NO_2 while above 675 K nitric oxide is reduced.

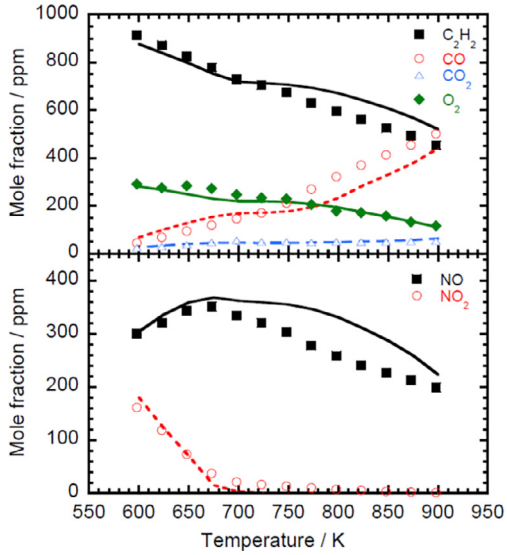

Fig. 6. Comparison of experimental and predicted concentration profiles as a function of the reactor temperature for the reducing experiment with C_2H_2/O_2 ($\lambda = 0.18$). The pressure was 59.6 bar and the reactor residence time was 8792/T (s · K). The inlet composition was 990 ppm C_2H_2, 470 ppm NO_x, 455 ppm O_2 (before reaction with NO in the inlet), and N_2 by difference. The symbols mark experimental data while solid lines denote model predictions obtained at isothermal conditions. In the modeling, the inlet NO_x was assumed to consist of 100 ppm NO and 370 ppm NO_2. Measured NO_2 was taken as the sum of NO_2, HONO, and $HONO_2$.

The modeling predictions are in good agreement with observations. They indicate that above 675 K NO is reduced to HCN by reaction with hydrocarbon radicals.

Figure 7 provides an overview of the major oxidation pathways for C_2H_2, according to the model. The solid lines denote pathways important across stoichiometries while the dashed lines denote pathways important mostly under reducing conditions. As expected, the initiation reaction is that of C_2H_2 with NO_2,

$$C_2H_2 + NO_2 \rightleftarrows CHCHO + NO \qquad (R1)$$

The CHCHO radical presumably reacts rapidly with O_2 or NO_2 to form glyoxal

$$CHCHO + O_2 \rightleftarrows OCHCHO + O$$

$$CHCHO + NO_2 \rightleftarrows OCHCHO + NO \qquad (R2)$$

or to feed into the carbon oxide pool,

$$CHCHO + O_2 \rightleftarrows HCO + CO_2 + H$$

Upon initiation, acetylene is oxidized also through the chain-propagating sequence,

$$C_2H_2 \xrightarrow{+OH} CHCHOH \xrightarrow{+O_2} OCHCHO + OH$$

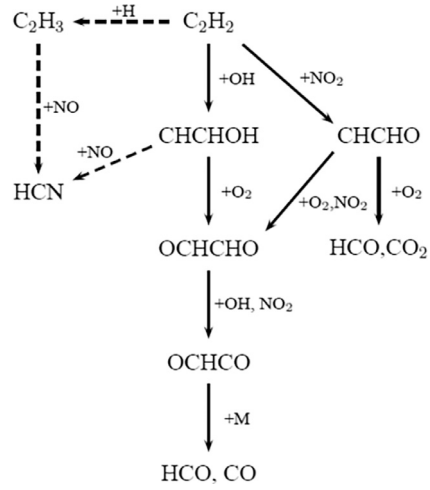

Fig. 7. Pathway diagram for conversion of acetylene and NO_x under the present conditions. Dashed lines denote reaction paths important mostly under reducing conditions.

which is the dominant oxidation pathway in the absence of nitrogen oxides [9,36]. Glyoxal reacts with OH and with NO_2 (R5) to form the OCHCO radical, which rapidly dissociates to yield HCO + CO.

Nitrogen dioxide is reduced to NO by reaction with C_2H_2 (R1) and CHCHO (R2). Reaction R1 is also the main sensitizing reaction. A smaller fraction of the nitric oxide may be recycled to NO_2 by reaction with HO_2. Under stoichiometric and reducing conditions, reactions of NO with C_2H_3 (R7) and CHCHOH (R8) feed into the cyanide pool. These two steps are both chain terminating and serve to inhibit the oxidation rate upon initiation.

4. Conclusions

The reaction of C_2H_2 with NO_2 has been studied theoretically. The calculated rate constant for the preferred channel, formation of a CHOCHON adduct, is compatible with the only experimental determination. The CHOCHON adduct is assumed to dissociate rapidly to form the triplet carbene CHCHO and NO. High pressure experiments for oxidation of C_2H_2 show that presence of NO_x serves both to sensitize and inhibit oxidation. Detailed chemical kinetic modeling confirms that $C_2H_2 + NO_2$ is the major initiation step, as well as the major sensitizing reaction. This reaction converts NO_2 to NO, which is then partly converted to HCN by reaction with C_2H_3 and CHCHOH. The latter reactions are both chain terminating and serve as the major inhibiting steps.

Acknowledgments

CL thanks the McNair Scholars Program for support. Computer facilities at UNT were purchased with NSF grant CHE-1531468. MA and MUA acknowledge MINECO and FEDER (project CTQ 2015–0334) for financial support. In addition, the work was financially supported by the Technical University of Denmark and the Danish Technical Research Council.

Supplementary material

Supplementary material associated with this article can be found, in the online version, at doi:10.1016/j.proci.2018.06.202

References

[1] R.P. Lindstedt, G. Skevis, *Combust. Sci. Technol.* 125 (1997) 73–137.
[2] J.M. Hay, R.G.W. Norrish, *Proc. R. Soc. Ser. A* 288 (1965) 17–38.
[3] T.M. Stevenson, C.F.H. Tipper, *Combust. Flame* 11 (1967) 35–48.
[4] J.M. Hay, D. Lyon, *Proc. Roy. Soc. Ser. A* 317 (1970) 1–20.
[5] A. Williams, D.B. Smith, *Chem. Rev.* 70 (1970) 267–293.
[6] Y.W. Tan, P. Dagaut, M. Cathonnet, J.C. Boettner, *Combust. Sci. Technol.* 102 (1994) 21–55.
[7] A.M. Tereza, V.G. Slutskii, E.S. Severin, *Russ. J. Phys. Chem. B* 3 (2009) 99–108.
[8] X. Shen, X. Yang, J. Santner, J. Sun, Y. Ju, *Proc. Combust. Inst.* 35 (2015) 721–728.
[9] J. Gimenez-Lopez, C.T. Rasmussen, H. Hashemi, M.U. Alzueta, Y. Gao, P. Marshall, C.F. Goldsmith, P. Glarborg, *Int. J. Chem. Kinet.* 172 (2016) 724–738.
[10] J.H. Thomas, *Trans. Faraday Soc.* 48 (1952) 1142–1149.
[11] W.G. Parker, H.G. Wolfhard, *Symp. (Int.) Combust.* 4 (1953) 420–428.
[12] B.A. Williams, L. Pasternack, *Combust. Flame* 111 (1997) 87–110.
[13] P. Dagaut, F. Lecomte, S. Chevailler, M. Cathonnet, *Fuel* 78 (1999) 1245–1252.
[14] P. Glarborg, M.U. Alzueta, K. Dam-Johansen, J.A. Miller, *Combust. Flame* 115 (1998) 1–27.
[15] P. Glarborg, *Proc. Combust. Inst.* 31 (2007) 77–98.
[16] J.H. Thomas, *Trans. Faraday Soc.* 49 (1953) 630–635.
[17] J.L. Sprung, H. Akimoto, J.N. Pitts Jr., *J. Am. Chem. Soc.* 96 (1974) 6549–6554.
[18] J.A. Montgomery Jr., M.J. Frisch, J.W. Ochterski, G.A. Petersson, *J. Chem. Phys.* 10 (1999) 2822–2827.
[19] Y. Zhao, D.G. Truhlar, *Theor. Chem. Acc.* 120 (2008) 215–241.
[20] I.M. Alecu, J. Zheng, Y. Zhao, D.G. Truhlar, *J. Chem. Theory Comput.* 6 (2010) 2872–2887.
[21] A. Halkier, T. Helgaker, P. Jorgensen, W. Klopper, H. Koch, J. Olsen, A.K. Wilson, *Chem. Phys. Lett.* 286 (1998) 243–252.
[22] J.A. Montgomery Jr., J.W. Ochterski, G.A. Petersson, *J. Chem. Phys.* 101 (1994) 5900–5909.
[23] M.J. Frisch, G.W. Trucks, H.B. Schlegel et al., 2013, Gaussian 09 (rev. D.01); Gaussian, Wallingford, CT.
[24] M.J. Frisch, G.W. Trucks, H.B. Schlegel et al. 2016. Gaussian 16 (rev. A.03); Gaussian, Wallingford, CT.
[25] J.R. Barker, T.L. Nguyen, J.F. Stanton et al. 2016. MultiWell-2016, University of Michigan, Ann Arbor, MI.
[26] J.W. Ochterski, G.A. Petersson, J.A. Montgomery, *J. Chem. Phys.* 104 (1996) 2598–2619.
[27] G.P.F. Wood, L. Radom, G.A. Petersson, E.C. Barnes, M.J. Frisch, J.A. Montgomery, *J. Chem. Phys.* 125 (2006) 094101–094116.
[28] T.J. Lee, P.R. Taylor, *Int. J. Quant. Chem., Quant. Chem. Symp.* S23 (1989) 199–207.
[29] J.C. Rienstra-Kiracofe, W.D. Allen, H.F. Schaefer III, *J. Phys. Chem. A* 104 (2000) 9823–9840.
[30] T.P.W. Jungkamp, J.H. Seinfeld, *J. Chem. Phys.* 107 (1997) 1513–1521.
[31] C.L. Rasmussen, J. Hansen, P. Marshall, P. Glarborg, *Int. J. Chem. Kinet.* 40 (2008) 454–480.
[32] J. Gimenez-Lopez, M.U. Alzueta, C.L. Rasmussen, P. Marshall, P. Glarborg, *Proc. Combust. Inst.* 33 (2011) 449–457.
[33] P. Glarborg, J.A. Miller, B. Ruscic, S.J. Klippenstein, *Prog. Energy Combust. Sci.* 67 (2018) 31–68.
[34] W.D. Geppert, A.J. Eskola, R.B. Timonen, L. Halonen, *J. Phys. Chem. A* 108 (2004) 4232–4238.
[35] F. Stribel, L.E. Jusinski, A. Fahr, J.B. Halpern, S.J. Klippenstein, C.A. Taatjes, *Phys. Chem. Chem. Phys.* 6 (2004) 2216–2223.
[36] M.U. Alzueta, M. Borruey, A. Callejas, A. Millera, R. Bilbao, *Combust. Flame* 152 (2008) 377–386.